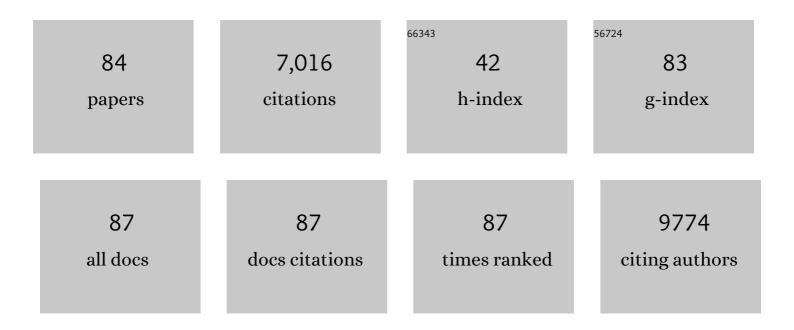
Dehong Chen

List of Publications by Year in descending order

Source: https://exaly.com/author-pdf/8554223/publications.pdf Version: 2024-02-01



#	Article	IF	CITATIONS
1	Crystal Facet Engineering of Singleâ€Crystalline TiC Nanocubes for Improved Hydrogen Evolution Reaction. Advanced Functional Materials, 2021, 31, 2008028.	14.9	17
2	Hierarchically Porous WO ₃ /CdWO ₄ Fiber-in-Tube Nanostructures Featuring Readily Accessible Active Sites and Enhanced Photocatalytic Effectiveness for Antibiotic Degradation in Water. ACS Applied Materials & Interfaces, 2021, 13, 21138-21148.	8.0	64
3	Rollâ€ŧoâ€Roll Processes for the Fabrication of Perovskite Solar Cells under Ambient Conditions. Solar Rrl, 2021, 5, 2100341.	5.8	22
4	Use of metamodels for rapid discovery of narrow bandgap oxide photocatalysts. IScience, 2021, 24, 103068.	4.1	17
5	Fluoride Perovskite (KNi _{<i>x</i>} Co _{1–<i>x</i>} F ₃) Oxygen-Evolution Electrocatalyst with Highly Polarized Electronic Configuration. ACS Applied Energy Materials, 2021, 4, 13425-13430.	5.1	12
6	Developing sustainable, high-performance perovskites in photocatalysis: design strategies and applications. Chemical Society Reviews, 2021, 50, 13692-13729.	38.1	97
7	Trace-Level Fluorination of Mesoporous TiO ₂ Improves Photocatalytic and Pb(II) Adsorbent Performances. Inorganic Chemistry, 2020, 59, 17631-17637.	4.0	9
8	The influence of ruthenium substitution in LaCoO ₃ towards bi-functional electrocatalytic activity for rechargeable Zn–air batteries. Journal of Materials Chemistry A, 2020, 8, 20612-20620.	10.3	32
9	Advancing Metalâ€Organic Frameworks toward Smart Sensing: Enhanced Fluorescence by a Photonic Metalâ€Organic Framework for Organic Vapor Sensing. Advanced Optical Materials, 2020, 8, 2000961.	7.3	36
10	Low-Temperature Solution-Processed Amorphous Titania Nanowire Thin Films for 1 cm ² Perovskite Solar Cells. ACS Applied Materials & Interfaces, 2020, 12, 11450-11458.	8.0	9
11	Ordered Mesoporous Graphitic Carbon/Iron Carbide Composites with High Porosity as a Sulfur Host for Li–S Batteries. ACS Applied Materials & Interfaces, 2019, 11, 13194-13204.	8.0	34
12	Tricomponent brookite/anatase TiO ₂ /g-C ₃ N ₄ heterojunction in mesoporous hollow microspheres for enhanced visible-light photocatalysis. Journal of Materials Chemistry A, 2018, 6, 7236-7245.	10.3	74
13	Solution-processed Zn2SnO4 electron transporting layer for efficient planar perovskite solar cells. Materials Today Energy, 2018, 7, 260-266.	4.7	30
14	Enhanced Photoelectrochemical Performances in Flexible Mesoscopic Solar Cells: An Effective Lightâ€ S cattering Material. ChemPhotoChem, 2018, 2, 986-993.	3.0	5
15	Enhanced Electrochromic Properties of WO ₃ Nanotree-like Structures Synthesized via a Two-Step Solvothermal Process Showing Promise for Electrochromic Window Application. ACS Applied Nano Materials, 2018, 1, 2552-2558.	5.0	84
16	The Formation of Defectâ€Pairs for Highly Efficient Visibleâ€Light Catalysts. Advanced Materials, 2017, 29, 1605123.	21.0	43
17	Monodisperse anatase titania microspheres with high-thermal stability and large pore size (â^¼80 nm) as efficient photocatalysts. Journal of Materials Chemistry A, 2017, 5, 3645-3654.	10.3	26
18	Colossal permittivity with ultralow dielectric loss in In + Ta co-doped rutile TiO ₂ . Journal of Materials Chemistry A, 2017, 5, 5436-5441.	10.3	123

#	Article	IF	CITATIONS
19	Recent progress in hybrid perovskite solar cells based on n-type materials. Journal of Materials Chemistry A, 2017, 5, 10092-10109.	10.3	136
20	Integrated planar and bulk dual heterojunctions capable of efficient electron and hole extraction for perovskite solar cells with >17% efficiency. Nano Energy, 2017, 32, 187-194.	16.0	23
21	Mesoporous TiO ₂ /g-C ₃ N ₄ Microspheres with Enhanced Visible-Light Photocatalytic Activity. Journal of Physical Chemistry C, 2017, 121, 22114-22122.	3.1	118
22	High Reversible Pseudocapacity in Mesoporous Yolk–Shell Anatase TiO ₂ /TiO ₂ (B) Microspheres Used as Anodes for Liâ€ i on Batteries. Advanced Functional Materials, 2017, 27, 1703270.	14.9	99
23	Colossal permittivity behavior and its origin in rutile (Mg1/3Ta2/3)xTi1-xO2. Scientific Reports, 2017, 7, 9950.	3.3	60
24	Thin Films of Tin Oxide Nanosheets Used as the Electron Transporting Layer for Improved Performance and Ambient Stability of Perovskite Photovoltaics. Solar Rrl, 2017, 1, 1700117.	5.8	69
25	Three-dimensional titanium oxide nanoarrays for perovskite photovoltaics: surface engineering for cascade charge extraction and beneficial surface passivation. Sustainable Energy and Fuels, 2017, 1, 1960-1967.	4.9	13
26	Solvent-Mediated Intragranular-Coarsening of CH ₃ NH ₃ PbI ₃ Thin Films toward High-Performance Perovskite Photovoltaics. ACS Applied Materials & Interfaces, 2017, 9, 31959-31967.	8.0	23
27	Chemical Bonding and Physical Trapping of Sulfur in Mesoporous Magnéli Ti ₄ O ₇ Microspheres for Highâ€Performance Li–S Battery. Advanced Energy Materials, 2017, 7, 1601616.	19.5	130
28	Stability Comparison of Perovskite Solar Cells Based on Zinc Oxide and Titania on Polymer Substrates. ChemSusChem, 2016, 9, 687-695.	6.8	101
29	N-doped Li ₄ Ti ₅ O ₁₂ nanoflakes derived from 2D protonated titanate for high performing anodes in lithium ion batteries. Journal of Materials Chemistry A, 2016, 4, 7772-7780.	10.3	39
30	Mesoporous Nitrogenâ€Modified Titania with Enhanced Dye Adsorption Capacity and Visible Light Photocatalytic Activity. ChemistrySelect, 2016, 1, 4868-4878.	1.5	20
31	Sub-100°C solution processed amorphous titania nanowire thin films for high-performance perovskite solar cells. Journal of Power Sources, 2016, 329, 17-22.	7.8	14
32	Optimizing semiconductor thin films with smooth surfaces and well-interconnected networks for high-performance perovskite solar cells. Journal of Materials Chemistry A, 2016, 4, 12463-12470.	10.3	28
33	Enhanced electrochromic performance of WO ₃ nanowire networks grown directly on fluorine-doped tin oxide substrates. Journal of Materials Chemistry C, 2016, 4, 10500-10508.	5.5	60
34	Perovskite Solar Cells: Solventâ€Mediated Dimension Tuning of Semiconducting Oxide Nanostructures as Efficient Charge Extraction Thin Films for Perovskite Solar Cells with Efficiency Exceeding 16% (Adv. Energy Mater. 7/2016). Advanced Energy Materials, 2016, 6, .	19.5	0
35	Solventâ€Mediated Dimension Tuning of Semiconducting Oxide Nanostructures as Efficient Charge Extraction Thin Films for Perovskite Solar Cells with Efficiency Exceeding 16%. Advanced Energy Materials, 2016, 6, 1502027.	19.5	52
36	Flowerlike WSe ₂ and WS ₂ microspheres: one-pot synthesis, formation mechanism and application in heavy metal ion sequestration. Chemical Communications, 2016, 52, 4481-4484.	4.1	81

#	Article	IF	CITATIONS
37	Extremely high arsenic removal capacity for mesoporous aluminium magnesium oxide composites. Environmental Science: Nano, 2016, 3, 94-106.	4.3	123
38	Chapter 7. Controlling the Photoanode Mesostructure for Dye-sensitized and Perovskite-sensitized Solar Cells. , 2016, , 292-323.		0
39	The Effect of the Scattering Layer in Dyeâ€Sensitized Solar Cells Employing a Cobaltâ€Based Aqueous Gel Electrolyte. ChemSusChem, 2015, 8, 3704-3711.	6.8	23
40	Temperature-induced modulation of mesopore size in hierarchically porous amorphous TiO ₂ /ZrO ₂ beads for improved dye adsorption capacity. Journal of Materials Chemistry A, 2015, 3, 3768-3776.	10.3	26
41	Thin Films of Dendritic Anatase Titania Nanowires Enable Effective Holeâ€Blocking and Efficient Lightâ€Harvesting for Highâ€Performance Mesoscopic Perovskite Solar Cells. Advanced Functional Materials, 2015, 25, 3264-3272.	14.9	101
42	Monodisperse mesoporous anatase beads as high performance and safer anodes for lithium ion batteries. Nanoscale, 2015, 7, 17947-17956.	5.6	21
43	Glucose-assisted synthesis of the hierarchical TiO ₂ nanowire@MoS ₂ nanosheet nanocomposite and its synergistic lithium storage performance. Journal of Materials Chemistry A, 2015, 3, 2762-2769.	10.3	142
44	Effect of cosolvents on the self-assembly of a non-ionic polyethylene oxide–polypropylene oxide–polyethylene oxide block copolymer in the protic ionic liquid ethylammonium nitrate. Journal of Colloid and Interface Science, 2015, 441, 46-51.	9.4	7
45	Effect of TiO ₂ microbead pore size on the performance of DSSCs with a cobalt based electrolyte. Nanoscale, 2014, 6, 13787-13794.	5.6	19
46	Understanding Solvothermal Crystallization of Mesoporous Anatase Beads by In Situ Synchrotron PXRD and SAXS. Chemistry of Materials, 2014, 26, 4563-4571.	6.7	37
47	Charge Transport in Photoanodes Constructed with Mesoporous TiO ₂ Beads for Dye-Sensitized Solar Cells. Journal of Physical Chemistry C, 2014, 118, 16635-16642.	3.1	8
48	Hierarchically Porous Titania Networks with Tunable Anatase:Rutile Ratios and Their Enhanced Photocatalytic Activities. ACS Applied Materials & Interfaces, 2014, 6, 13129-13137.	8.0	73
49	Mesoporous titania beads for flexible dye-sensitized solar cells. Journal of Materials Chemistry C, 2014, 2, 1284-1289.	5.5	16
50	Versatile inorganic-organic hybrid WO x -ethylenediamine nanowires: Synthesis, mechanism and application in heavy metal ion adsorption and catalysis. Nano Research, 2014, 7, 903-916.	10.4	59
51	Surfaceâ€Metastable Phaseâ€Initiated Seeding and Ostwald Ripening: A Facile Fluorineâ€Free Process towards Spherical Fluffy Core/Shell, Yolk/Shell, and Hollow Anatase Nanostructures. Angewandte Chemie - International Edition, 2013, 52, 10986-10991.	13.8	99
52	Methyl orange removal by combined visible-light photocatalysis and membrane distillation. Dyes and Pigments, 2013, 98, 106-112.	3.7	64
53	Mesoporous Titanium Zirconium Oxide Nanospheres with Potential for Drug Delivery Applications. ACS Applied Materials & Interfaces, 2013, 5, 10926-10932.	8.0	43
54	Engineering of Monodisperse Mesoporous Titania Beads for Photocatalytic Applications. ACS Applied Materials & Interfaces, 2013, 5, 9421-9428.	8.0	49

#	Article	IF	CITATIONS
55	Recent Progress in the Synthesis of Spherical Titania Nanostructures and Their Applications. Advanced Functional Materials, 2013, 23, 1356-1374.	14.9	195
56	Amine-Functionalized Titania-based Porous Structures for Carbon Dioxide Postcombustion Capture. Journal of Physical Chemistry C, 2013, 117, 9747-9757.	3.1	28
57	Enhanced Photocatalytic Activity: Macroporous Electrospun Mats of Mesoporous Au/TiO ₂ Nanofibers. ChemCatChem, 2013, 5, 2646-2654.	3.7	28
58	Construction of nanostructured electrodes on flexible substrates using pre-treated building blocks. Applied Physics Letters, 2012, 100, .	3.3	31
59	Sensitization of nickel oxide: improved carrier lifetime and charge collection by tuning nanoscale crystallinity. Chemical Communications, 2012, 48, 9885.	4.1	60
60	Spiky Mesoporous Anatase Titania Beads: A Metastable Ammonium Titanateâ€Mediated Synthesis. Chemistry - A European Journal, 2012, 18, 13762-13769.	3.3	27
61	Facile Synthesis of Monodisperse Mesoporous Zirconium Titanium Oxide Microspheres with Varying Compositions and High Surface Areas for Heavy Metal Ion Sequestration. Advanced Functional Materials, 2012, 22, 1966-1971.	14.9	73
62	Flexible dye-sensitized solar cells containing multiple dyes in discrete layers. Energy and Environmental Science, 2011, 4, 2803.	30.8	41
63	Noble Metalâ€Modified Porous Titania Networks and their Application as Photocatalysts. ChemCatChem, 2011, 3, 1763-1771.	3.7	28
64	Effect of Mesoporous TiO2 Bead Diameter in Working Electrodes on the Efficiency of Dye-Sensitized Solar Cells. ChemSusChem, 2011, 4, 1498-1503.	6.8	40
65	Dualâ€Function Scattering Layer of Submicrometer‣ized Mesoporous TiO ₂ Beads for Highâ€Efficiency Dye‣ensitized Solar Cells. Advanced Functional Materials, 2010, 20, 1301-1305.	14.9	385
66	Dye-Sensitized Solar Cells Employing a Single Film of Mesoporous TiO ₂ Beads Achieve Power Conversion Efficiencies Over 10%. ACS Nano, 2010, 4, 4420-4425.	14.6	412
67	Synthesis of Monodisperse Mesoporous Titania Beads with Controllable Diameter, High Surface Areas, and Variable Pore Diameters (14â^23 nm). Journal of the American Chemical Society, 2010, 132, 4438-4444.	13.7	405
68	Mesoporous Anatase TiO ₂ Beads with High Surface Areas and Controllable Pore Sizes: A Superior Candidate for Highâ€Performance Dyeâ€Sensitized Solar Cells. Advanced Materials, 2009, 21, 2206-2210.	21.0	926
69	Mesoporous Fe2O3 microspheres: Rapid and effective enrichment of phosphopeptides for MALDI-TOF MS analysis. Journal of Colloid and Interface Science, 2008, 318, 315-321.	9.4	69
70	Nitrogen-containing carbon spheres with very large uniform mesopores: The superior electrode materials for EDLC in organic electrolyte. Carbon, 2007, 45, 1757-1763.	10.3	330
71	Nitrogen enriched mesoporous carbon spheres obtained by a facile method and its application for electrochemical capacitor. Electrochemistry Communications, 2007, 9, 569-573.	4.7	255
72	Synthesis and phase behaviors of bicontinuous cubic mesoporous silica from triblock copolymer mixed anionic surfactant. Microporous and Mesoporous Materials, 2007, 105, 34-40.	4.4	26

#	Article	IF	CITATIONS
73	Anionic surfactant induced mesophase transformation to synthesize highly ordered large-pore mesoporous silica structures. Journal of Materials Chemistry, 2006, 16, 1511.	6.7	130
74	Highly Ordered Mesoporous Silicon Carbide Ceramics with Large Surface Areas and High Stability. Advanced Functional Materials, 2006, 16, 561-567.	14.9	199
75	Synthesis of Large-Pore Periodic Mesoporous Organosilica (PMO) with Bicontinuous Cubic Structure ofla–3dSymmetry. Chemistry Letters, 2005, 34, 182-183.	1.3	24
76	Titania and Mixed Titania/Aluminum, Gallium, or Indium Oxide Spheres: Sol-Gel/Template Synthesis and Photocatalytic Properties. Advanced Functional Materials, 2005, 15, 239-245.	14.9	82
77	Nonionic Block Copolymer and Anionic Mixed Surfactants Directed Synthesis of Highly Ordered Mesoporous Silica with Bicontinuous Cubic Structure. Chemistry of Materials, 2005, 17, 3228-3234.	6.7	91
78	Micrometer-to-Nanometer Replication of Hierarchical Structures by Using a Surface Sol–Gel Process. Angewandte Chemie - International Edition, 2004, 43, 2746-2748.	13.8	96
79	An Easy Route for the Synthesis of Ordered Three-Dimensional Large-Pore Mesoporous Organosilicas withIm-3mSymmetry. Chemistry Letters, 2004, 33, 1132-1133.	1.3	12
80	Hydrothermal synthesis and characterization of octahedral nickel ferrite particles. Powder Technology, 2003, 133, 247-250.	4.2	90
81	Inorganic Macroporous Films from Preformed Nanoparticles and Membrane Templates: Synthesis and Investigation of Photocatalytic and Photoelectrochemical Properties. Advanced Functional Materials, 2003, 13, 789-794.	14.9	102
82	Hollow-structured hematite particles derived from layered iron (hydro)oxyhydroxide–surfactant composites. Journal of Materials Chemistry, 2003, 13, 2266-2270.	6.7	53
83	Preparation and characteristics of sol–gel derived Zn2SiO4 doped with Ni2+. Inorganic Chemistry Communication, 2002, 5, 482-486.	3.9	19
84	Solvothermal synthesis of α-Fe2O3 particles with different morphologies. Materials Research Bulletin, 2001, 36, 1057-1064.	5.2	32